Microfluid Nanofluid
DOI 10.1007/s10404-013-1152-6

RESEARCH PAPER

Mass production of highly monodisperse polymeric nanoparticles by parallel flow focusing system

Xianjie Kang · Chunxiong Luo · Qiong Wei · Chunyang Xiong · Qian Chen · Ying Chen · Qi Ouyang

Received: 8 November 2012 / Accepted: 6 February 2013
© Springer-Verlag Berlin Heidelberg 2013

Abstract Nanoparticles can be prepared through nanoprecipitation by mixing polymers dissolved in organic solvents with anti-solvents. However, due to the inability to precisely control the mixing processes during the synthesis of polymeric nanoparticles, its application is limited by a lack of homogeneous physicochemical properties. Here, we report that this obstacle can be overcome through rapid and controlled mixing by parallel flow focusing outside the microfluidic channels. Using the nanoprecipitation of methoxyl poly-(ethylene glycol)–poly-(lactic-co-glycolic acid) (MPEG–PLGA) block copolymers as an example, we prove that our parallel flow focusing method is a robust and predictable approach to synthesize highly monodisperse polymeric nanoparticles, and demonstrate that it improves the production speed of nanoparticles by an order of magnitude or more compared with previous microfluidic systems. Possible aggregation on the surface of PDMS wall and clogging of microchannels reported previously were avoided in the synthesis process of our method. This work is a typical application combining the advantages of microfluidics with nanoparticle technologies, suggesting that microfluidics may find applications in the development and mass production of polymeric nanoparticles with high monodispersity in large-scale industrial production field.

Keywords Mass production · Polymeric nanoparticles · High monodispersity · Microfluidics · Parallel flow focusing

Electronic supplementary material The online version of this article (doi:10.1007/s10404-013-1152-6) contains supplementary material, which is available to authorized users.

X. Kang · C. Luo (✉) · Q. Ouyang
The State Key Laboratory for Artificial Microstructures and Mesoscopic Physics, School of Physics, Peking University, Beijing, China
e-mail: pkuluocx@pku.edu.cn

C. Luo · Q. Ouyang (✉)
Center for Quantitative Biology, Academy for Advanced Interdisciplinary Studies, Peking University, Beijing, China
e-mail: qi@pku.edu.cn

Q. Wei · C. Xiong
Department of Biomedical Engineering, Peking University, Beijing, China

Q. Chen
College of Environmental Sciences and Engineering, Peking University, Beijing, China

Y. Chen
RSinno Pharmaceuticals LLC, Beijing, China

1 Introduction

Over the past decade, microfluidics has attracted enormous attention in different application fields because of its various advantages over traditional technologies (deMello and deMello 2004; deMello 2006) such as precise operations of fluid, high mixing speed, and massively parallel processing with very small amounts of reagents. One of the application field is the development of inorganic nanoparticles (Shestopalov et al. 2004; Chan et al. 2005; Wagner and Kohler 2005; Krishnadasan et al. 2007; Lo et al. 2010; Jahn et al. 2010) and microparticles (Xu et al. 2005) which has been greatly promoted by the combination of microfluidics and particle technologies. In the past few years, there has been an increasing interest in the development of organic nanoparticles by microfluidics, especially polymeric nanoparticles, for drug delivery (Soppimath et al. 2001; Peer et al. 2007; Davis et al. 2008; Farokhzad and Langer

Published online: 26 February 2013

2009; Riehemann et al. 2009). Biodegradable and biocompatible polymeric nanoparticles composed of poly-(lactide-co-glycolide)–b-poly(ethylene glycol) (PLGA–PEG) block copolymers have been previously synthesized (Karnik et al. 2008; Rhee et al. 2011) by different groups using nanoprecipitation (Quintanar-Guerrero et al. 1998) for various biomedical applications (Gref et al. 1994; Davaran et al. 2006; Farokhzad et al. 2006; Zhang et al. 2007). Optimal physicochemical characteristics of PLGA–PEG nanoparticles, such as incorporating a variety of targeting agents, high payload of drug molecules and controlled drug release (Gref et al. 1994; Farokhzad and Langer 2009) have shown considerable promise allowing meaningful applications including drug loading, encapsulation and release (Karnik et al. 2008) and cancer treatment (Farokhzad et al. 2004, 2006; Gu et al. 2008).

Nanoparticles can be prepared by mixing and nanoprecipitation of polymers dissolved in organic solvents such as acetonitrile with anti-solvents such as water. However, the inability to precisely control the mixing processes by conventional approach of bulk mixing results in highly polydisperse particles; it compromises the physicochemical properties of the nanoparticle product. Several groups have previously used PLGA–PEG block copolymers to prepare nanoparticles using 2D hydrodynamic flow focusing on microfluidic channels (Karnik et al. 2008; Valencia et al. 2010), in which the polymer stream in acetonitrile was horizontally focused by water sheath streams. However, the adsorption of the hydrophobic polymer onto the surface of mcirofluidic channel (Wu et al. 2005; Wong and Ho 2009) causes aggregation of polymer nanoparticles with high molecular weight or high concentration, which may lead to increased internal pressure in the microfluidic channels, resulting in irreversible failure of device and lack of robustness of operation. A better approach to prevent the nanoparticles from aggregation on the PDMS walls and clogging in the microchannels is the 3D hydrodynamic flow focusing technique, in which the polymer stream was both horizontally and vertically focused.

In recent years, a variety of 3D focusing systems with intrinsic 3D structures such as vertical chimneys (Wolff and Perch-Nielsen 2003), horizontal nozzles (Huang et al. 2006) and 3D channel network (Scott and 2008) have been reported. However, complex fabrication processes and limited reproducibility rate inevitably resulted in huge costs. Not long ago, a method of 3D fluid operation in a single layer as microfluidic drifting (Mao et al. 2007; Lim et al. 2011) was proposed. Despite its facile fabrication, it only worked for limited conditions, such as relatively low sample flow rates and high Reynolds numbers. More recently, another 3D focusing system composed of a monolithic single layer with three sequential inlets for vertical focusing followed by a conventional cross junction for horizontal focusing (Rhee et al. 2011) has been suggested. Excessive accurately drilled inlets and complex yet precise control for multiple fluids were required for the stable focusing. Besides, only relatively low sample flow rates were forbore in a single channel, which may easily cause instability of flow focusing and low throughput. Taking into account the possible aggregation with the 2D hydrodynamic flow focusing systems, complications and low throughputs with the 3D hydrodynamic flow focusing systems, a platform which can be easily fabricated and operated for stable mass production of polymeric nanoparticles without aggregation and clogging is urgently demanded.

The method presented in this paper involves the formation of MPEG–PLGA nanoparticles by rapid mixing of polymers dissolved in acetonitrile with water in a controlled nanoprecipitation process. Structure of our device composed of three-tier PDMS microchannels where the middle layer is for the polymer stream and both the top and the bottom layers are for the water stream. MPEG–PLGA nanoparticles were synthesized through self-assembly of block copolymers outside the PDMS microchannels by our parallel flow focusing method. This ensured isolation of the precipitating polymer from the PDMS wall. We used confocal microscopy image to confirm the presence and the shape of the focused polymer stream and accurately calculated the mixing time by measurement of the size of the focused polymer stream. We applied our device to synthesize polymeric nanoparticles at various molecular weights ($MPEG_{5K}$–$PLGA_{27K}$, $MPEG_{5K}$–$PLGA_{55K}$ and $MPEG_{5K}$–$PLGA_{95K}$, respectively) and investigate the robustness of nanoprecipitation by our device.

2 Experimental

2.1 Solution preparation of polymer precursors

For synthesis of polymeric MPEG–PLGA nanoparticles, block solids of MPEG–PLGA (Jinan Daigang Biomaterial Co., Ltd, China) at molecular weights of $MPEG_{5K}$–$PLGA_{27K}$, $MPEG_{5K}$–$PLGA_{55K}$ and $MPEG_{5K}$–$PLGA_{95K}$ were dissolved in acetonitrile to form solution at concentrations of 10, 30 and 50 mg/mL, respectively. A vortex oscillator was used to fully dissolve them.

2.2 Design and fabrication of microfluidic device

Our device was fabricated with poly-(dimethylsiloxane) (PDMS) using the standard soft lithographic technique (see Supporting Information). Figure 1a shows the masks for different layers for polymeric nanoparticle synthesis. Figure 1b shows a side view of the architecture of our microfluidic device design. This design consists of the top

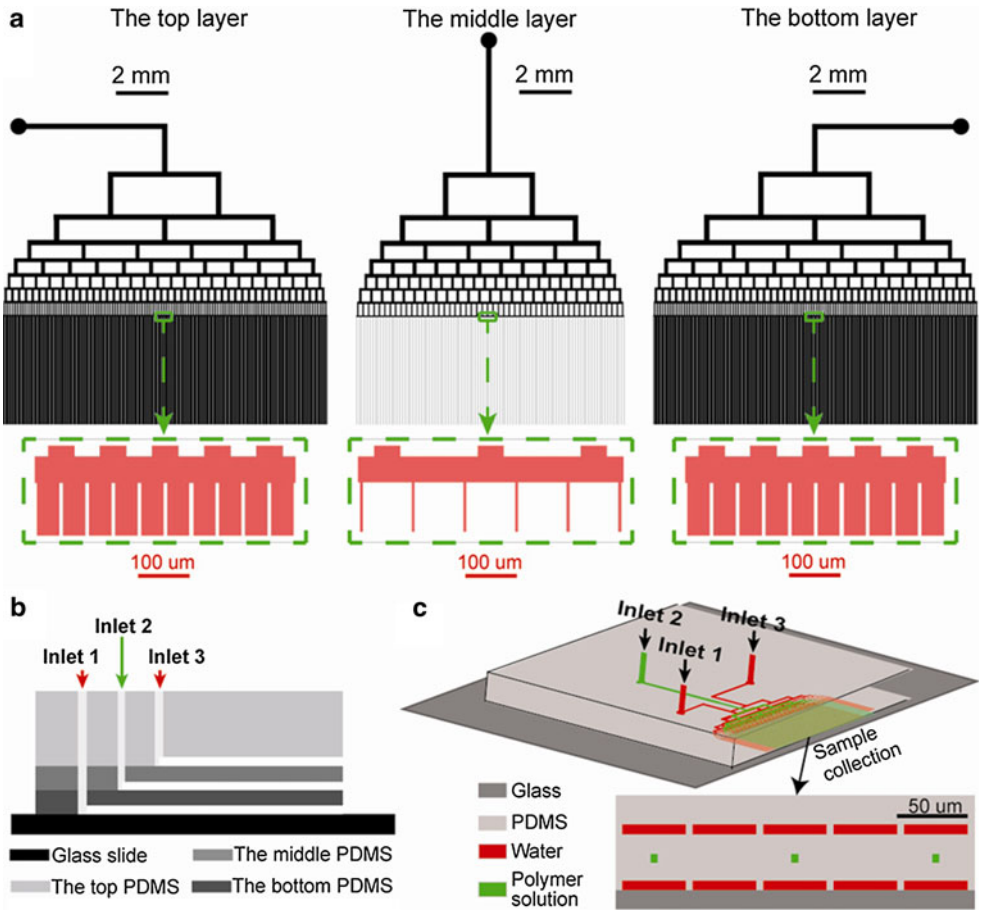

Fig. 1 **a** The masks for the top, the middle and the bottom layer, respectively. For each layer, microchannels from the inlets to outlets are designed as a tree structure, which equally divides into two tributary channels from one flow channel, and then equally divide into three tributary channels, until dividing into 100 (the middle layer)/240 (the top and bottom layers) tributary channels as their respective outlets. The figures surrounded by *dotted lines* are enlarged details of each mask at the outlets. Typical outlets for polymer channels in the middle layer have a width of 5 μm (interval is 95 μm and line period is 100 μm; length of the line is 1 cm, resulting in 100 outlets). For the water channels in the top and bottom layers, the typical outlets have a width of 45 μm (interval is 5 μm and line period is 50 μm; length of the line is 1.2 cm, resulting in 240 outlets). The total width (including intervals) of 100 polymer solution outlets is 1 cm, which can be covered by the total width (including intervals) of 240 water outlets (1.2 cm). **b** A side view of the architecture of our device design consisting of three layers of microchannels (not to scale). **c** A schematic image of our microfluidic device design for parallel flow focusing (not to scale). The figure to which pointed by a *black arrow* shows the enlarged cross-sectional view of outlets. Sample of nanoparticles was collected in a disposable plastic dish. In both **b** and **c**, *inlet 2* is for the polymer stream and *inlet 1* and *inlet 3* are for the water stream

layer of PDMS, the middle layer of PDMS, the bottom layer of PDMS, and a glass slide. There are grooves of tree structure at the bottom of each layer of PDMS. Three layers of PDMS are bonded together according to the graphic alignment. Grooves of the top layer of PDMS and the middle layer of PDMS form the top layer microchannels; grooves of the middle layer of PDMS and the bottom layer of PDMS form the middle layer microchannels; and grooves of the bottom layer of PDMS and the glass slide form the bottom layer microchannels. There are 100 outlets (5 μm width and 6 μm height) for the polymer stream in the middle layer and 240 outlets (45 μm width and 7 μm height) for the water stream in the top and bottom layers. Meanwhile, three inlets interlinked with the corresponding microchannels of each layer are set up in the upper surface of the top layer of PDMS for injection of different solutions. More details for the three-tier PDMS microfluidic device fabrication can be found in Supporting Information. Figure 1c shows a schematic image of our microfluidic device design. Polymer solution was injected into the middle layer of channels by inlet 2 and water was injected into the top/bottom layer of channels by inlet 1/3 using syringe pumps. The polymer stream was focused vertically by the water sheath streams with higher flow rates after flowing out from the outlets, resulting in solvent exchange as acetonitrile diffused out of the focused stream and water diffused into the focused stream. Thus, self-assembly of the nanoparticles was triggered by rapidly mixing outside the

microchannels. Sample of nanoparticles was collected in a disposable plastic dish.

2.3 Fluid control

For nanoparticle synthesis experiments, two 10.00-mL syringes for water injection were mounted on two syringe pumps (Baoding Longer Precision Pump Co., Ltd, China), respectively, while a 1-mL syringe for polymer solution injection was mounted on another syringe pump of the same type. Water and polymer flow rates at inlets were maintained at 5.0 and 1.0 mL/h, respectively. For synthesis of nanoparticles by parallel flow focusing, the injected volume of polymer solution at different molecular weights ($MPEG_{5K}$–$PLGA_{27K}$, $MPEG_{5K}$–$PLGA_{55K}$ and $MPEG_{5K}$–$PLGA_{95K}$, respectively) and different concentrations (10, 30 and 50 mg/mL, respectively) was set to be a constant as 0.4 mL for each run. For comparison with the conventional synthesis by bulk mixing, the same volume of polymer solution was pipetted into deionized water and stirred fully for the same time duration as in microfluidic synthesis experiments.

To survey whether mixing time had significant influence on the particle size distribution of nanoparticles in the nanoparticle synthesis experiments by our device, polymer flow rates were typically chosen to be 0.5, 1.0 and 2.0 mL/h at molecular weights of $MPEG_{5K}$–$PLGA_{55K}$ and concentration of 50 mg/mL while water flow rates were always maintained at 5.0 mL/h without change. Meanwhile, to survey whether bonding among three-layer channels according to graphic random alignment had effect on the robustness of our chips or not, three randomly selected chips were used in the experiments at molecular weights of $MPEG_{5K}$–$PLGA_{95K}$ and polymer solution concentration of 30 mg/mL.

2.4 Synthesis of MPEG–PLGA nanoparticles

Figure 2a shows the scene of operation of our microfluidic device. Fluidic connection was achieved by inserting 0.80 mm OD needles which were connected to 0.80 ID PTFE tubing. In the nanoparticle synthesis experiments, the chip connected to needles and tubing was placed flat in a disposable plastic dish. Some amount (~5 mL) of deionized water was placed at the flow focus position to maintain much steadier laminar flow. Before liquid inhalation, tubing and syringes were rinsed for more than three times (with acetonitrile for the polymer stream and with deionized water for the aqueous stream) and the residual liquid was removed. Two syringe pumps for water injection had been operating for about 3 min before starting the syringe pump for polymer solution injection and the former continued for about 2 min after the latter had stopped

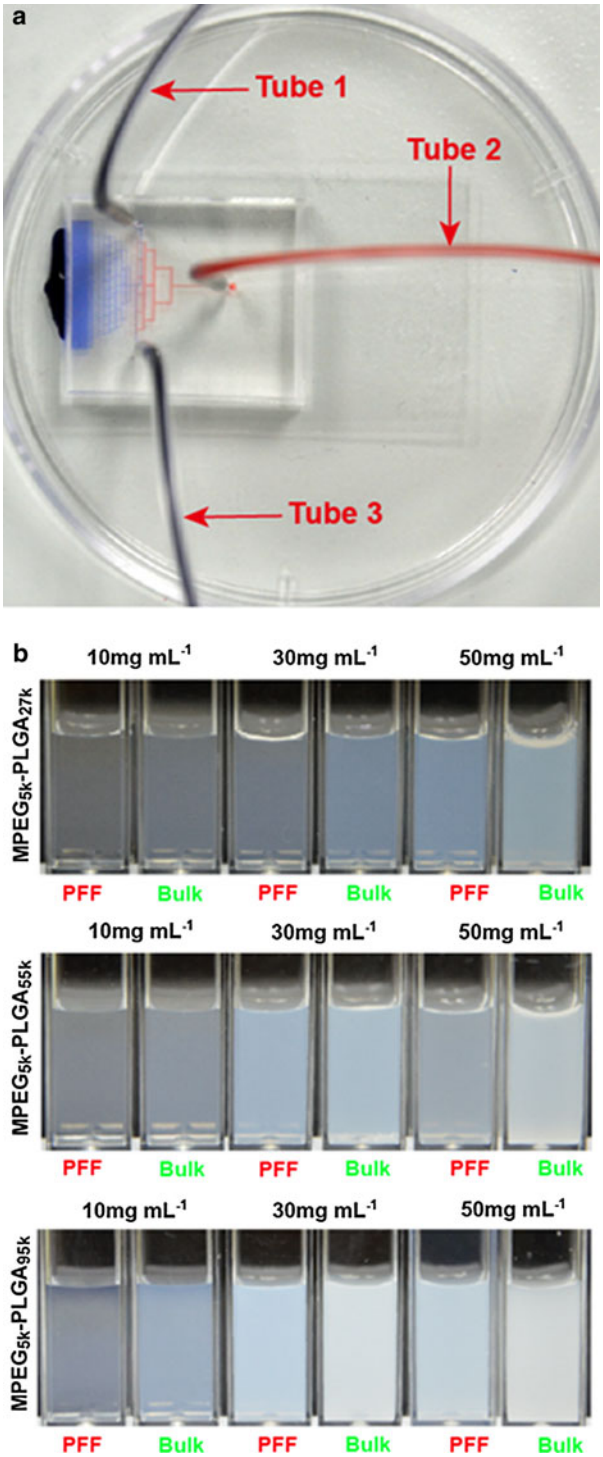

Fig. 2 **a** Photo of the microfluidic device which is under operation. The channels of polymer flow are dyed with *red ink* and the channels of adjacent water streams are dyed with *blue ink*. *Tube 2* is for the polymer solution injection and *tube 1* and *tube 3* are for water injection. **b** Photos of nanoparticle solutions obtained by parallel flow focusing (*PFF*) and bulk synthesis. We can roughly compare the average size of nanoparticles in different solutions through their opacity. Clear solutions have relatively small nanoparticles and opaque solutions contain relatively large particles up to several microns (color figure online)

automatically, which was to ensure steady laminar flow and prevent possible adsorption and aggregation on the PDMS surface of the fluid outlet cross section. For each experiment, the resulting suspension in dish was collected in a 15-mL disposable centrifuge tube. Deionized water was then added into the tube to the total volume of 12 mL. Thus, volume fraction of acetonitrile was about 3.3 %, appropriate for preventing slight deviations of the measured size. The suspension of constant volume was stored and used for further measuring and analysis. In bulk mixing, 0.4 mL of polymer solution was pipetted into 12 mL of deionized water and stirred fully during the same time as spent in microfluidic synthesis experiments. Figure 2b shows photos of nanoparticle solutions prepared by parallel flow focusing (PFF) and bulk synthesis. They provide us with direct visualization of collected nanoparticle solutions that contain MPEG–PLGA particles with various sizes synthesized from different molecular weight polymer precursors at various concentrations. Larger particles can reflect more light, so the solution with larger particles looks opaque. Nanoparticle solutions obtained by both parallel flow focusing and bulk synthesis are relatively clear only at very low concentrations or very small polymer molecular weights. However, at high concentrations or large polymer molecular weights, nanoparticle solutions prepared by bulk mixing are much more opaque compared with those prepared by parallel flow focusing method, indicating that the latter synthesized relatively smaller particles.

2.5 Particle sizing

Dynamic light scattering was used to measure the particle diameter indirectly. Particle sizing was performed using dynamic light scattering with Zetasizer Nano ZS90 (Malvern Instruments Ltd., UK). For each measurement, 1 mL of the sample was loaded in a disposable low-volume cuvette. More than three measurements were performed on each sample. To obtain more accurate measurement result, suspension sample was appropriately diluted to ensure that mass fraction of nanoparticles was between 1/10,000 and 1/1,000. Meanwhile, all measurements were performed at acetonitrile concentrations of $\leq$3.3 % acetonitrile to ensure that any observed variation in particle size was not due to the solvent. Z-average sizes and size distributions were obtained using Dispersion Technology Software 5.00 (Malvern Instruments Ltd., UK) as the average of more than three measurements.

2.6 Transmission electron microscopy (TEM) imaging

TEM imaging was performed with a field emission transmission electron microscope Tecnai F30 (FEI Company, Netherlands) at an acceleration voltage of 300 kV. To prepare the TEM sample, 15 μL of the nanoparticle suspension (0.33 − 1.67 mg/mL) sample was dropped onto a 230-mesh formvar–carbon coated copper grid. The sample was blotted away after 30 s incubation and then the grid was negatively stained with 3 % uranyl acetate aqueous solution for 5 min at the room temperature. Uranyl acetate aqueous solution was then blotted away and the grid was washed three times with distilled water and dried at 40 °C before being imaged. For every sample, various fields were imaged to confirm the monodispersity of the resulting nanoparticles at different magnifications.

2.7 Confocal imaging

Confocal imaging experiments were carried out on a Nikon A1R MP Multiphoton Confocal microscope (Nikon Instruments Inc, China). Microfluidic device with corresponding tubing for inlets as used in the nanoparticles synthesis experiments was mounted on the stage of the microscope. Fluorescein-anti-human IgG (H + L) (with small diffusion constant) solution (dissolved in PBS) was used as a substitute for the polymer solution at flow rate of 1.0 mL/h, while water stream (PBS solution) of both sides at flow rate of 5.0 mL/h was not labeled. For the focused polymer streams by parallel flow focusing method, a z-stack of 57 images was taken at 0.85 μm per z-sectioning step with 20× objective and a z-stack of 150 images was taken at 0.20 μm per z-sectioning step with 60× objective. The wavelength of laser used for confocal imaging was 488 nm.

3 Results and discussion

Cross-sectional view of outlets of fluid is presented in Fig. 3a. Typical outlets for polymer channels in the middle layer have a width of 5 μm (line period is 100 μm and length is 1 cm, resulting in 100 outlets) and a height of 6 μm. For the water channels in the top and bottom layers, the typical outlets have a width of 45 μm (line period is 50 μm and length is 1.2 cm, resulting in 240 outlets) and a height of 7 μm. PDMS thickness is 20 μm for both the middle and bottom layer. Flow rates at inlets were maintained at 5.0 mL/h (V_{H_2O}), 1.0 mL/h (V_{poly}) and 5.0 mL/h (V_{H_2O}) for the top, the middle and the bottom layer stream, respectively. The mixing time (τ_{mix}) for parallel flow focusing can be estimated from the diffusion timescale as:

$$\tau_{mix} \sim \frac{(h/2)^2}{D} \quad (1)$$

where D is diffusion constant of acetonitrile in water ($D = 10^{-9}$ m^2/s), h is the height of the focused polymer stream after flowing out from the channel outlet. In the experiments, confocal microscopy was used to confirm the presence and the shape of the focused polymer stream and

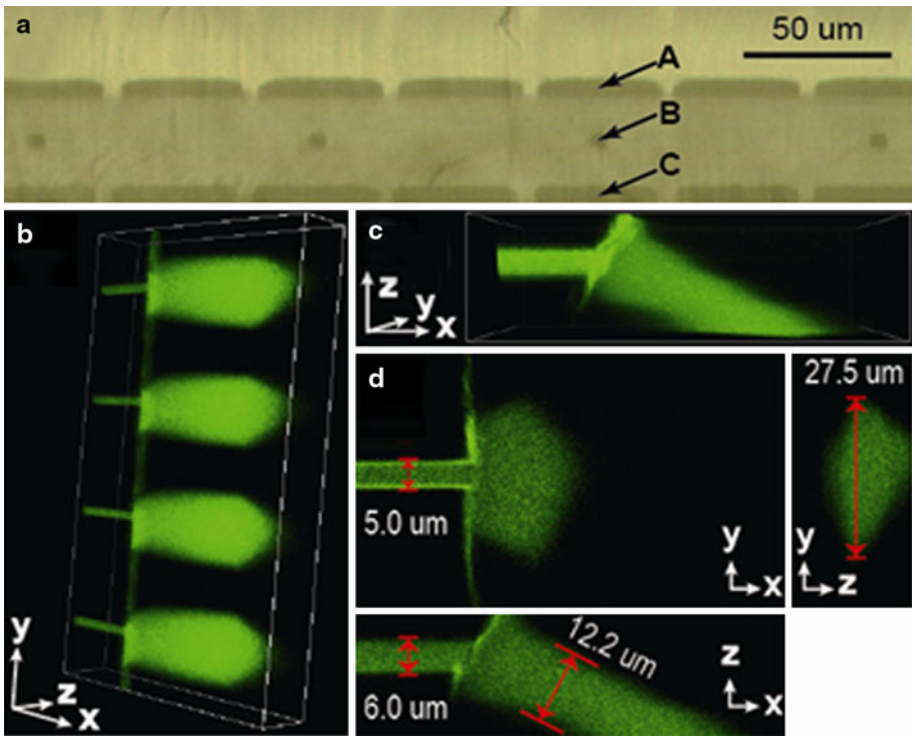

Fig. 3 **a** Cross-sectional view of outlets of fluid (*scale bar* 50 μm). Outlet *B* corresponds to the polymer stream and outlet *A* and *C* correspond to the water stream. **b** Confocal microscopy images composed of a z-stack of 57 images obtained with 20× objective. The image shows 3D view of the focused polymer streams by parallel flow focusing before and after flowing out from the outlets of the middle layer. **c** Confocal microscopy image composed of a z-stack of 150 images obtained with 60× objective. The image shows 3D view of a focused polymer stream. **d** Confocal microscopy images showing cross-sectional views corresponding to **c**. The *top left panel* shows a top view of one of the 150 images of the focused polymer stream. The width of outlet for polymer solution is measured to be 5 μm, which is consistent with our designed size. The *top right panel* shows a front view of the focused polymer stream. The last width of the focused polymer stream broadened to 27.5 from 5 μm after flowing out from the outlet. The *bottom panel* shows a side view of the focused polymer stream. The measured outlet height of 6 μm is consistent with our designed size. The last height of the focused polymer stream is 12.2 μm in the stable parallel flow focusing

accurately calculate the mixing time. We used fluorescein-anti-human IgG (with small diffusion constant) labeled stream (dissolved in PBS) as a substitute for the polymer solution at flow rate of 1.0 mL/h while both adjacent water streams (PBS solution) were at flow rate of 5.0 mL/h. In Fig. 3b, confocal microscopy images composed of a z-stack of 57 images obtained with 20× objective show 3D view of the focused polymer streams by parallel flow focusing before and after flowing out from the outlets of the middle layer. The performance of different focused polymer streams was highly consistent. Functionality of the two adjacent water flows was clarified to be as designed by a control experiment (see Supporting Information). Figure 3c shows confocal microscopy image composed of a z-stack of 150 images obtained with 60× objective, showing 3D view of one of the focused polymer streams. In Fig. 3d, confocal microscopy images show cross-sectional views corresponding to Fig. 3c. The three panels show top view of one of the 150 images, front view and side view of the focused polymer stream, respectively. The measured outlet widths of 5 μm and height of 6 μm are consistent with our designed size. In the stable parallel flow focusing, the last width and height of the focused polymer stream after flowing out from the outlet broadened to 27.5 and 12.2 μm, respectively. Thus, Eq. (1) predicts a mixing time of ∼37 ms in our device. Besides, focusing zones (width and depth of the focused polymer flow) in different cases were compared by confocal imaging and simulations to obtain the trend of focusing zones as the polymer flow rate changes (see Supporting Information).

The characteristic nanoprecipitate time scale for a typical copolymers has been found to be in the range of 26–60 ms for concentrations ranging from 0.1 to 0.65 % w/w (Johnson and Prud'homme 2003). When the mixing of polymer solvent and anti-solvent is nearly complete and self-assembly of copolymers into nanoparticles occurs, the nanoparticle sizes become independent of mixing time if mixing occurs faster than the characteristic nanoprecipitate time scale of nanoparticles (Karnik et al. 2008). This was true in our device. In the experiments, the MPEG–PLGA was dissolved in acetonitrile solvent; water was used as the anti-solvent. It was found that diameters of nanoparticles

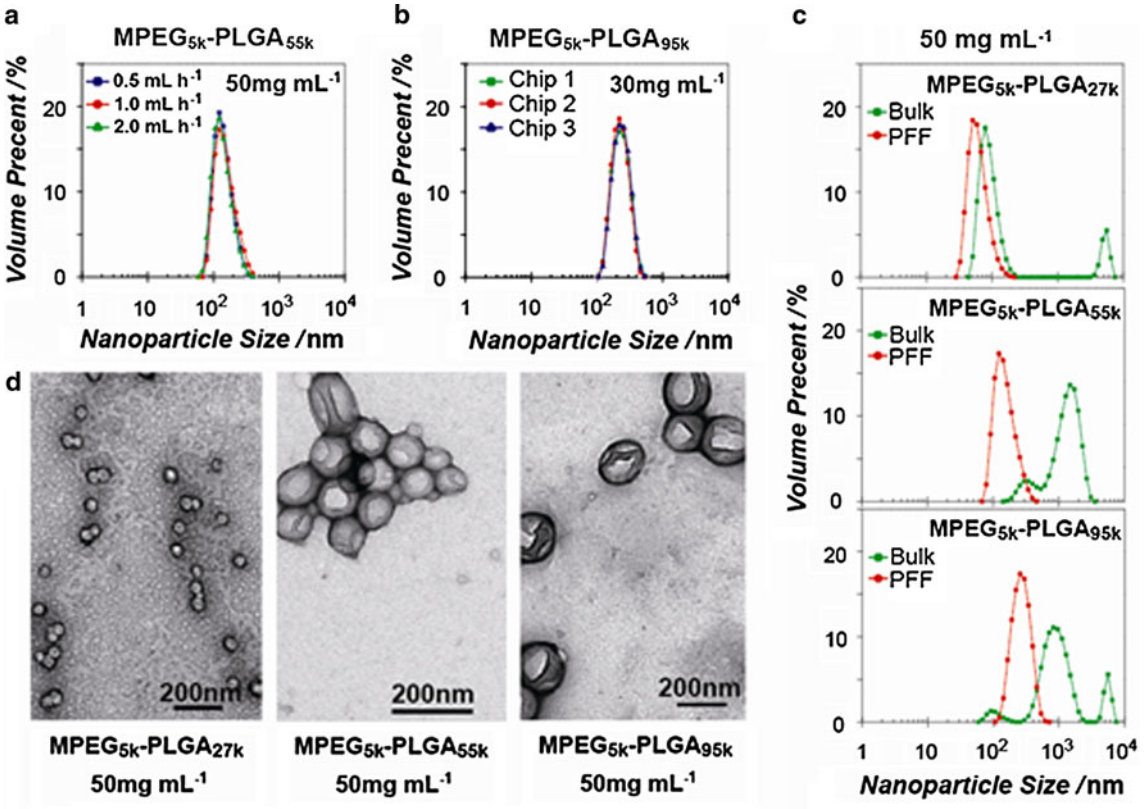

Fig. 4 **a** Size distributions by volume fraction of nanoparticles synthesized from $MPEG_{5K}$–$PLGA_{55K}$ by parallel flow focusing for the concentration of 50 mg/mL at different polymer flow rates (0.5, 1.0 and 2.0 mL/h, respectively) and adjacent water flow rates of 5.0 mL/h remaining unchanged. **b** Size distributions by volume fraction of nanoparticles synthesized from $MPEG_{5K}$–$PLGA_{95K}$ by parallel flow focusing at concentration of polymer solution of 30 mg/mL using three randomly selected chips. The polymer flow rates are all 1.0 mL/h and the adjacent water flow rates are 5.0 mL/h. **c** Size distributions by volume fraction of nanoparticles synthesized from $MPEG_{5K}$–$PLGA_{27K}$, $MPEG_{5K}$–$PLGA_{55K}$ and $MPEG_{5K}$–$PLGA_{95K}$, respectively, using parallel flow focusing and bulk mixing methods for the concentration of polymer solution of 50 mg/mL. For the parallel flow focusing method, the polymer flow rates are all 1.0 mL/h and the adjacent water flow rates are 5.0 mL/h. **d** TEM images of nanoparticles prepared from $MPEG_{5K}$–$PLGA_{27K}$, $MPEG_{5K}$–$PLGA_{55K}$ and $MPEG_{5K}$–$PLGA_{95K}$ at 50 mg/mL in acetonitrile by parallel flow focusing. Flow rate of polymer stream is 1.0 mL/h and flow rates of both water streams are 5.0 mL/h. Average nanoparticle sizes are 50, 130, 200 nm, respectively

prepared by a series of gradually increasing mixing time scales (yet shorter than the characteristic nanoprecipitate time scale) basically remain the same (Johnson and Prud'homme 2003). Figure 4a shows the size distributions by volume fraction of nanoparticles synthesized from $MPEG_{5K}$–$PLGA_{55K}$ by parallel flow focusing for the precursor concentration of 50 mg/mL at different polymer flow rates [0.5 mL/h ($0.5V$), 1.0 mL/h (V) and 2.0 mL/h ($2V$), respectively] and water flow rates of 5.0 mL/h both for the top and bottom layer channels remaining unchanged. Assume that the mixing time corresponding to the three different polymer flow rates were $\tau_{0.5v}$, τ_v, and τ_{2v}, respectively. Meanwhile, the characteristic aggregation time scale for MPEG–PLGA copolymers to self-assemble into nanoparticles was assumed to be τ_{agg}. It was found that the larger the polymer flow rate at inlet was, the higher the height of the focused polymer stream would be (see Supporting Information). The height of the focused polymer stream would become higher given a larger polymer flow rate when water stream rates of both sides were kept the same, resulting in a larger mixing time τ_{mix}. No significant differences were found in size distributions by volume fraction when polymer flow rate varied from 0.5 mL/h ($0.5V$) to 1.0 mL/h (V) and to 2.0 mL/h ($2V$). Thus, we can obtain the relationship among different mixing time and the characteristic aggregation time scale for MPEG–PLGA copolymers as:

$$\tau_{0.5v} < \tau_v < \tau_{2v} \leq \tau_{agg}. \quad (2)$$

It was confirmed that the mixing time (τ_{mix}) in our experiments was shorter than the aggregation time (τ_{agg}) of nanoparticles, i.e., acetonitrile and water had fully mixed before self-assembly of MPEG–PLGA copolymers into nanoparticles.

To check whether misalignment of channels has any effect on the robustness of our chips, three randomly

selected chips were used in the experiments with molecular weights of $MPEG_{5K}$–$PLGA_{95K}$ and polymer solution concentration of 30 mg/mL. Figure 4b shows there is no significant difference in size distributions by volume fraction of nanoparticles synthesized with different chips. This comparison verifies excellent robustness of our chips; the misalignment does not influence the results.

Monodispersity and size of nanoparticles prepared by our method were compared with those by conventional bulk mixing. Figure 4c shows the size distributions by volume fraction of nanoparticles synthesized from various MPEG–PLGA molecular weights (25, 55, and 95 kDa) prepared by parallel flow focusing and bulk mixing method. At the same concentration of 50 mg/mL, parallel flow focusing method consistently synthesized smaller nanoparticles with a relatively low polydispersity regardless of polymer molecular weight, while the bulk mixing method produced particles with high polydispersity of extremely large size (>1,000 nm) for all polymer molecular weights. These experimental results indicate that parallel flow focusing is a more robust method to reproducibly synthesize highly monodisperse nanoparticles regardless of both molecular weights of polymer and concentrations of polymer solution. We also found that size distributions of MPEG–PLGA nanoparticles did not change too much with the variety of concentrations of polymer solution from low (10 mg/mL) to high (50 mg/mL) for the same small molecular weight (27, 55 kDa). However, an obvious increase in size was presented as polymer molecular weights increase from low (27 kDa) to high (95 kDa) for the same concentration (see Supporting Information). This phenomenon indicates that nanoparticle size may be relatively sensitive to polymer molecular weights compared to concentrations of polymer solution.

To further verify the monodispersity and the size of nanoparticles produced by parallel flow focusing method, transmission electron microscopy (TEM) imaging was performed with a Tecnai F30 field emission transmission electron microscope. TEM images of MPEG–PLGA nanoparticles prepared from polymers with different molecular weights by parallel flow focusing are presented in Fig. 4d. It shows that our method produces monodisperse nanoparticles of average sizes ranging from 50 to 200 nm. Size measurements of the nanoparticles by dynamic light scattering were basically consistent with the TEM imaging results.

4 Conclusion

Herein, we presented a novel, facile and robust approach to efficiently synthesize highly monodisperse MPEG–PLGA nanoparticles of average sizes ranging from 50 to 200 nm regardless of molecular weight of polymer and concentration of polymer solution. We demonstrated that parallel flow focusing in our device yielded smaller nanoparticles with high monodispersity because of predictable control over the mixing process of microfluidic synthesis of nanoparticles. Possible aggregation on the surface of PDMS wall and clogging of microchannels reported previously (Wu et al. 2005; Wong and Ho 2009; Rhee et al. 2011) were avoided in the synthesis process since self-assembly of nanoparticles occurred outside the PDMS microchannels, which ensured isolation of the precipitating polymer from the PDMS wall and thus resulted in good reproducibility. More significantly, the production speed of nanoparticles in this device was improved by an order of magnitude as compared to the production efficiency reported previously (Karnik et al. 2008; Rhee et al. 2011). In this paper, we just designed 100 outlets for the polymer stream in the middle layer of PDMS for demonstration. One can certainly further improve the production speed of nanoparticles by two orders of magnitude or more by increasing the number of the outlets. Meanwhile, our design does not require excessively precise flow control, yet has operational simplicity and excellent experimental stability. We believe this innovative technique can serve as a good base for the large-scale industrial production of polymeric nanoparticles with high monodispersity.

Acknowledgments We would like to thank W.K. Wang, X.J. Zhu, G.W. Si, Y.G. Wang for helpful discussions. This work is partially supported by the NSF of China (10721403, 11074009, 11174012), the MOST of China (2009CB918500) and the NFFTBS of China (J0630311).

References

Chan EM, Alivisatos AP et al (2005) High-temperature microfluidic synthesis of CdSe nanocrystals in nanoliter droplets. J Am Chem Soc 127(40):13854–13861

Davaran S, Rashidi MR et al (2006) Adriamycin release from poly(lactide-co-glycolide)-polyethylene glycol nanoparticles: synthesis, and in vitro characterization. Int J Nanomed 1(4):535–539

Davis ME, Chen Z et al (2008) Nanoparticle therapeutics: an emerging treatment modality for cancer. Nat Rev Drug Discov 7(9):771–782

deMello AJ (2006) Control and detection of chemical reactions in microfluidic systems. Nature 442(7101):394–402

deMello J, deMello A (2004) Microscale reactors: nanoscale products. Lab Chip 4(2):11N–15N

Farokhzad OC, Langer R (2009) Impact of nanotechnology on drug delivery. ACS Nano 3(1):16–20

Farokhzad OC, Jon SY et al (2004) Nanoparticle–aptamer bioconjugates: a new approach for targeting prostate cancer cells. Cancer Res 64(21):7668–7672

Farokhzad OC, Cheng JJ et al (2006) Targeted nanoparticle–aptamer bioconjugates for cancer chemotherapy in vivo. Proc Natl Acad Sci USA 103(16):6315–6320

Gref R, Minamitake Y et al (1994) Biodegradable long-circulating polymeric nanospheres. Science 263(5153):1600–1603

Gu F, Zhang L et al (2008) Precise engineering of targeted nanoparticles by using self-assembled biointegrated block copolymers. Proc Natl Acad Sci USA 105(7):2586–2591

Huang S-H, Tan W-H et al (2006) A monolithically three-dimensional flow-focusing device for formation of single/double emulsions in closed/open microfluidic systems. J Micromech Microeng 16(11):2336–2344

Jahn A, Stavis SM et al (2010) Microfluidic mixing and the formation of nanoscale lipid vesicles. ACS Nano 4(4):2077–2087

Johnson BK, Prud'homme RK (2003) Mechanism for rapid self-assembly of block copolymer nanoparticles. Phys Rev Lett 91(11):118302 (Epub 2003 Sep 11)

Karnik R, Gu F et al (2008) Microfluidic platform for controlled synthesis of polymeric nanoparticles. Nano Lett 8(9):2906–2912

Krishnadasan S, Brown RJC et al (2007) Intelligent routes to the controlled synthesis of nanoparticles. Lab Chip 7(11):1434–1441

Lim J-M, Kim S-H et al (2011) Liquid-liquid fluorescent waveguides using microfluidic-drifting-induced hydrodynamic focusing. Microfluid Nanofluid 10(1):211–217

Lo CT, Jahn A et al (2010) Controlled self-assembly of monodisperse niosomes by microfluidic hydrodynamic focusing. Langmuir 26(11):8559–8566

Mao X, Waldeisen JR et al (2007) "Microfluidic drifting"—implementing three-dimensional hydrodynamic focusing with a single-layer planar microfluidic device. Lab Chip 7(10):1260–1262

Peer D, Karp JM et al (2007) Nanocarriers as an emerging platform for cancer therapy. Nat Nanotechnol 2(12):751–760

Quintanar-Guerrero D, Allemann E et al (1998) Preparation techniques and mechanisms of formation of biodegradable nanoparticles from preformed polymers. Drug Dev Ind Pharm 24(12):1113–1128

Rhee M, Valencia PM et al (2011) Synthesis of size-tunable polymeric nanoparticles enabled by 3D hydrodynamic flow focusing in single-layer microchannels. Adv Mater 23(12):H79–H83

Riehemann K, Schneider SW et al (2009) Nanomedicine—challenge and perspectives. Angew Chem (Int Ed 48(5):872–897

Scott R, Sethu P et al (2008) Three-dimensional hydrodynamic focusing in a microfluidic Coulter counter. Rev Sci Instrum 79(4)

Shestopalov I, Tice JD et al (2004) Multi-step synthesis of nanoparticles performed on millisecond time scale in a microfluidic droplet-based system. Lab Chip 4(4):316–321

Soppimath KS, Aminabhavi TM et al (2001) Biodegradable polymeric nanoparticles as drug delivery devices. J Control Release 70(1–2):1–20

Valencia PM, Basto PA et al (2010) Single-step assembly of homogenous lipid–polymeric and lipid–quantum dot nanoparticles enabled by microfluidic rapid mixing. ACS Nano 4(3):1671–1679

Wagner J, Kohler JM (2005) Continuous synthesis of gold nanoparticles in a microreactor. Nano Lett 5(4):685–691

Wolff A, Perch-Nielsen IR et al (2003) Integrating advanced functionality in a microfabricated high-throughput fluorescent-activated cell sorter. Lab Chip 3(1):22–27

Wong I, Ho C-M (2009) Surface molecular property modifications for poly(dimethylsiloxane) (PDMS) based microfluidic devices. Microfluid Nanofluid 7(3):291–306

Wu DP, Luo Y et al (2005) Multilayer poly(vinyl alcohol)-adsorbed coating on poly(dimethylsiloxane) microfluidic chips for biopolymer separation. Electrophoresis 26(1):211–218

Xu S, Nie Z et al (2005) Generation of monodisperse particles by using microfluidics: control over size, shape, and composition. Angew Chem Int Ed 44(25):724–728

Zhang H, Tumarkin E et al (2007) Exploring microfluidic routes to microgels of biological polymers. Macromol Rapid Commun 28(5):527–538